ISSN 0010-9525, Cosmic Research, 2013, Vol. 51, No. 6, pp. 401–412. © Pleiades Publishing, Ltd., 2013.
Original Russian Text © N.S. Nikolaeva, Yu.I. Yermolaev, I.G. Lodkina, 2013, published in Kosmicheskie Issledovaniya, 2013, Vol. 51, No. 6, pp. 443–454.

Modeling the Time Behavior of the D_{st} Index during the Main Phase of Magnetic Storms Generated by Various Types of Solar Wind

N. S. Nikolaeva, Yu. I. Yermolaev, and I. G. Lodkina

Space Research Institute, Russian Academy of Sciences, ul. Profsoyuznaya 84/32, Moscow, 117997 Russia

Received December 24, 2012

Abstract—Results of modeling the time behavior of the D_{st} index at the main phase of 93 geomagnetic storms ($-250 < D_{st} \le -50$ nT) caused by different types of solar wind (SW) streams: magnetic clouds (MC, 10 storms), corotating interaction regions (CIR, 31 storms), the compression region before interplanetary coronal ejections (Sheath before ICME, 21 storms), and "pistons" (Ejecta, 31 storms) are presented. The "Catalog of Large-Scale Solar Wind Phenomena during 1976–2000" (ftp://ftp.iki.rssi.ru/pub/omni/) created on the basis of the OMNI database was the initial data for the analysis. The main phase of magnetic storms is approximated by a linear dependence on the main parameters of the solar wind: integral electric field *sumEy*, dynamic pressure P_d, and fluctuation level *sB* in IMF. For all types of SW, the main phase of magnetic storms is better modeled by individual values of the approximation coefficients: the correlation coefficient is high and the standard deviation between the modeled and measured values of D_{st} is low. The accuracy of the model in question is higher for storms from MC and is lower by a factor of ~2 for the storms from other types of SW. The version of the model with the approximation coefficients averaged over SW type describes worse variations of the measured D_{st} index: the correlation coefficient is the lowest for the storms caused by MC and the highest for the Sheath- and CIR- induced storms. The model accuracy is the highest for the storms caused by Ejecta and, for the storms caused by Sheath, is a factor of ~1.42 lower. Addition of corrections for the prehistory of the development of the beginning of the main phase of the magnetic storm improves modeling parameters for all types of interplanetary sources of storms: the correlation coefficient varies within the range from $r = 0.81$ for the storms caused by Ejecta to $r = 0.85$ for the storms caused by Sheath. The highest accuracy is for the storms caused by MC. It is, by a factor of ~1.5, lower for the Sheath-induced storms.

DOI: 10.1134/S0010952513060038

1. INTRODUCTION

This paper is dedicated to modeling the time behavior of the D_{st} index at the main phase of magnetic storms induced by various types of solar wind (SW) streams. It presents a continuation of the series of publications [1–7] dedicated to study of the process of generation of magnetic storms by various types of solar wind streams. Based on our results that the D_{st} index at the main phase of a magnetic storm is well approximated by the linear function of the integral of the B_z component of the interplanetary magnetic field (IMF) (substituted at the data processing by summation sumB_z) or of the integral of the electric field E_y (sumE_y) [1–3], we showed in our previous publications [4–6] that the linear character of the D_{st} dependence on sumE_y on the average is observed for all types of the solar wind, but differs by values of the coefficients. For several types of magnetic storms related mainly to the compression regions (CIR, Sheath), the magnetic storm intensity increases strongly (D_{st} decreases) in the subgroup of points at the main phase with high dynamic pressure. On the background of the D_{st} dependence on sumE_y at the main phase of magnetic storms, a very weak dependence on the fluctuation level *sB* in IMF is observed almost for all types of flows [5, 6].

Note that the linear character of the D_{st} dependence of the main phase of a magnetic storm on the integral of E_y (sumE_y) follows from [8] in the case of neglecting the term related to the decay of the ring current at the main phase. This result has been confirmed in a series of publications (without any selection of magnetic storms by the type of their source in the solar wind) (see, for example, [9–11] and references therein).

On the basis of these results, we have earlier performed a modeling of the D_{st}-index behavior during the main phase of magnetic storms induced by magnetic clouds (MC). It was assumed that the linear relation between D_{st} and the integral of the electric field E_y plays a key role in development of the main phase, whereas the dependencies on pressure P_d and variations s*B* in IMF were believed to be small [7]. The results obtained showed that the proposed approaches make it possible not only to describe satisfactorily the relation of interplanetary parameters of MC to the dynamics of the D_{st} index but to create forecasting schemes for prediction of D_{st} values 1–2 hours in advance.

Currently, there exist a vast number of publications dedicated to the modeling of magnetic storms and their prediction (see, for example, [8, 12–19] and references therein). Various methods are used to predict D_{st} index, for example the method of filters, when the solar wind–magnetosphere system is considered as a *black box*, artificial neuron networks, and nonlinear auto-regression schemes (see, for example, [20–32]).

In the overwhelming majority of papers, the type of SW stream which generated storms is not taken into account. However, there are publications which show that various types of SW streams lead to different disturbances in the magnetosphere (see, for example, [33–47, 1–6]).

In one of the recent publications [32], a comparison is presented of 6 different models [8, 13, 14, 16, 27, 28, 31] by the results of their prediction of 63 strong magnetic storms (minimum $D_{st} \le -100$ nT) which were split to four groups depending on the type of their source in SW. Twenty seven sMC-induced storms (MC with the preceding rapid shock wave), 18 SH events (the compression region Sheath), 8 CIR events (corotating interaction regions), 10 nonMC events (i.e., the ICME type but the field structure differs from MC, i.e., Ejecta) were analyzed separately. As a result, it was shown that the TL model [27, 28] is the best for prediction of the D_{st} index during strong magnetic storms for any type of source in SW, and also for 63 strong storms and all 139 moderate and strong magnetic storms without separation according to the type of sources in SW.

We use the traditional description of the storm dynamics by the D_{st} index for which there are long homogeneous series of data in spite of the fact that various current systems of the magnetosphere and ionosphere could contribute to its value (see, for example, [48, 49]).

In this paper, a possibility of approximation of the main phase of magnetic storms generated by four types of solar wind streams by linear dependence on the solar wind parameters: the integral electric field sumE_y, the dynamic pressure P_d, and the fluctuation level sB in the IMF. The correctness of these assumptions is checked by the comparison of the calculation results to experimental data and results of modeling in other publications.

The main aim of this paper is to reveal the differences in the development of the main phase of magnetic storms, the source of which are various types of solar wind streams (CIR, Sheath, MC, and Ejecta), by comparison of results of modeling the main phase for various types of storms and by estimation of the contributions of the main parameters of the SW into the D_{st} index at the main phase of the storm.

2. INITIAL DATA AND METHOD

On the basis of the OMNI database for the period 1976–2000 [50], we identified large-scale types of the solar wind (see "Catalog of Large-Scale Solar Wind Phenomena during 1976–2000" at ftp://ftp.iki.rssi.ru/pub/omni/ and in [51]). The method of identification of large-scale streams of the solar wind comprises a comparison of each point of the OMNI database [50] to a set of threshold criteria for the key parameters of the solar wind and IMF and is described in detail in [51].

In this paper, magnetic storms for which there were gaps in measurements in the OMNI database making it possible to calculate three parameters (E_y, P_d, and sB) in the period of the main phase of a magnetic storm were excluded from the analysis. Moreover, to reduce the error and improve the approximation, the storms having the approximation coefficients which lie outside two standard deviations from the mean value were also excluded [7]. As a result, 93 magnetic storms ($-250 < D_{st} \le -50$ nT) induced by 4 types of solar wind streams (CIR (31 storms), Sheath (21 storms), MC (10 storms), and Ejecta (31 storms)) were selected for the analysis.

It was shown in several previous publications [52–54] that the strongest (on average) magnetic storms caused by sporadic (i.e., conglomerate Sheath+ICME) streams are related to nonisolated events when the distance between consecutive interplanetary events (between the arrivals of interplanetary shock waves and SSC) was less then 40 hours. In this paper, we did not analyze the distance between SW events, but we sorted storms and compared them to the source in SW in the following way. If the time between the D_{st} minimums was longer than 24 hours, the storms were considered as isolated. If the time between the D_{st} minimums was less than 24 hours (multistep storm), both minimums were considered as one storm with the intensity equal to the minimum value of D_{st}. There were a few percent of such single storms with two minimums during 24 hours. Therefore, their contribution to the total dependence is insignificant, whereas the D_{st} level from the prehistory is accounted for by the coefficient c_0) (see below).

While modeling the main phase of a magnetic storm, a linear approximation of the D_{st}-index value of the main phase of a magnetic storm is taken into account by three parameters of the solar wind: the integral of the convective electric field of the solar wind sumE_y, the dynamic pressure P_d, and interplanetary magnetic field variations sB [7]:

$$D_{st}(i) = c_0 + c_E \cdot \mathrm{sum}E_y(i) + c_P \cdot P_d(i) + c_B \cdot sB(i),$$
$$\mathrm{sum}E_y(i) = \sum_{k=1}^{k=i} E_y(k), \quad (1)$$

where i is the current point of the storm phase (varies from $i = 1$ in the beginning of the phase to $i = im$ at the last point of the phase (in $D_{st\,\min}$)) and the summation in sumE_y is performed in terms of k (from the beginning of the storm at the $k = 1$ point to the current point of the phase $k = i$). The coefficients c_0, c_E, c_P, and c_B

Table 1. The mean and median values of the approximation coefficients at the main phase of a magnetic storm, mean SW parameters to the value of the D_{st} index for four types of SW streams

Type of SW	MC 10 storms	Sheath 21 storms	CIR 31 storms	Ejecta 31 storms
$\langle c_0 \rangle$, nT median	**−13.77 ± 14.4** **−11**	**−13.1 ± 28.8** **−18**	**−28.7 ± 30.5** **−32**	**−30.7 ± 23.1** **−32**
$\langle c_E \rangle$, nT/mV m^{-1} h median	**−2.55 ± 0.75** **−2.4**	**−3.2 ± 1.6** **−3.3**	**−2.82 ± 1.1** **−2.8**	**−2.3 ± 1.0** **−2.2**
$\langle c_P \rangle$, nT/nPa median	−0.92 ± 2.9 **1**	0.97 ± 3.3 **1**	**3.3 ± 3.7** **2.6**	**2.8 ± 3.9** **2.8**
$\langle c_B \rangle$, dimensionless median	1.28 ± 3.3 **0**	−0.8 ± 1.8 **−1**	−0.19 ± 1.96 **0**	−0.2 ± 2.1 **0**
$\langle \mathrm{sum}E_y \rangle$	**16.24 ± 9.78**	**16.4 ± 13.5**	**13.3 ± 10.4**	**15.6 ± 11.8**
$\langle c_E \rangle \cdot \langle \mathrm{sum}E_y \rangle$	**−41.41**	**−52.5**	**−37.5**	**−35.9**
$\langle P_d \rangle$	**3.62 ± 2.27**	**5.7 ± 5.7**	**5.5 ± 3.1**	**4.3 ± 2.7**
$\langle c_p \rangle \cdot \langle P_d \rangle$	**−3.33**	**5.5**	**18.15**	**12.04**
$\langle sB \rangle$	**3.07 ± 2.4**	**5.1 ± 4.1**	**5.4 ± 3.3**	**3.6 ± 2.5**
$\langle c_B \rangle \cdot \langle sB \rangle$	**3.93**	**−4.08**	**−1.03**	**−0.72**

were estimated by the standard least squares method (at the same time, the number of points during the main phase should be larger than the number of unknowns, i.e., $im > 4$). The coefficients c_E, c_P, and c_B determine the value of the linear relation of the D_{st} index to the integral of convective electric field of the solar wind sumE_y, dynamic pressure P_d, and variations in the interplanetary magnetic field sB. The c_0 coefficient is related mainly to the prehistory of the D_{st} index prior to the magnetic storm commencement, because the storm can "start" from any initial value of the index both due to the beginning of a new storm during the recovery phase of the previous storm (a decrease in the level relative to "zero") and due to the presence of the storm sudden commencement (SSC) related to the arrival of the shock wave prior to the storm commencement (an increase in the level).

For each type of magnetic storm, the modeling of the main phase was performed in three steps. First, the individual approximation coefficients (c_0, c_E, c_P, c_B) are determined for the main phase of a particular storm of each type. Then the approximation coefficients of the main phase of a storm are averaged according to the type of SW ($\langle c_0 \rangle$, $\langle c_E \rangle$, $\langle c_P \rangle$, $\langle c_B \rangle$) and for the version of the model, the contribution to D_{st} during the main phase from particular SW parameters entering equation (1) is estimated. On the basis of the analysis of these versions of the model, for each type of SW, third version of the model is created due to the corrections taking into account the prehistory of the development of the main phase of a magnetic storm by the calculation of a linear function relating the average value of the D_{st} index over three points (the first point of the main phase and two previous points) and the value of c_0 [7].

Each version of the model was estimated by two parameters (for example, [12]): 1) the linear correlation coefficient (r) between the measured D_{st} and modeled $D_{st\ mod}$ values (how correctly the model describes the real variations in the D_{st} index) and 2) the standard deviation (σ) between the measured value of D_{st} and the value calculated using the model $D_{st\ mod}$ (how strong are the differences between the measured D_{st} and $D_{st\ mod}$ values calculated in the model, i.e., the modeling accuracy).

3. RESULTS

3.1. Estimation of Contribution of Various SW Parameters to the Approximation of the Main Phase of a Magnetic Storm Induced by Various Streams of SW

Table 1 shows the mean and median values of the approximation coefficients of the main phase of a magnetic storm ($\langle c_0 \rangle$, $\langle c_E \rangle$, $\langle c_P \rangle$, $\langle c_B \rangle$), mean SW parameters ($\langle \mathrm{sum}E_y \rangle$, $\langle P_d \rangle$, $\langle sB \rangle$) and contributions of these parameters ($\langle c_E \rangle \cdot \langle \mathrm{sum}E_y \rangle$, $\langle c_P \rangle \cdot \langle P_d \rangle$, $\langle c_B \rangle \cdot \langle sB \rangle$) to the value of the D_{st} index for four types of SW streams (MC, Sheath, CIR, and Ejecta). Although the scatter of individual coefficients is sufficiently high (which one can see in the standard deviations of the values) their mean values are close to the median ones, that is, the scatter of the individual values is fairly symmetrical relative to the mean values. In all cases, when the standard deviation exceeds the mean (median) value, the statistical significance of the corresponding coefficient is not high enough to draw a reliable conclusion on the basis of this coefficient, so we show such results as a possible hypothesis which requires further checks.

The $\langle c_0 \rangle$ coefficient is negative for all types of SW (that is, it always "reduces" D_{st} which is natural due to the definition of the magnetic storm beginning and its main phase). The $\langle c_0 \rangle$ coefficient varies by a factor of ~2.4 from the maximum value for MC and Sheath (high level of D_{st} from which the storm begins possibly due to SSC prior to the storm beginning) to the minimum value for CIR and Ejecta. However, the scatter in values of c_0 (for particular storms) is high and comparable to the value of the mean value $\langle c_0 \rangle$ itself and even exceeds it (for the storms caused by Sheath).

The coefficient $\langle c_E \rangle$ is determined by how strong the electric field (the sumE_y parameter) changes the D_{st} index at the main phase of storms. The $\langle c_E \rangle$ coefficient is negative and reduces the D_{st} value for all four types of storms. The strongest and weakest reduction in D_{st} from the integral electric field is observed for the storms caused by Sheath and Ejecta, respectively (it varies by a factor of ~1.4). The strongest decrease in D_{st} is observed for the Sheath-induced storms and it leads under the same value of the field to more rapid decrease in D_{st} than for other types of SW.

The contribution of E_y into D_{st} (i.e., the value of $\langle c_E \rangle \cdot \langle \text{sum}E_y \rangle$) is the largest and the smallest for the storms caused by Sheath and Ejecta, respectively. The maximum difference in the contribution of this term reaches a factor of ~1.4 and is determined mainly by the $\langle c_E \rangle$ coefficient but not by the $\langle \text{sum}E_y \rangle$ value.

The $\langle c_P \rangle$ coefficient determines the contribution of the dynamic pressure into the value of D_{st} at the main phase. On average, the $\langle c_P \rangle$ value varies from the minimum value for the MC-induced storms (i.e., slight intensification of the storm or a decrease in D_{st}) to the maximum value for the CIR-induced storms (i.e., weakening of the storm or increase in D_{st}). However, the strong scatter in the c_P values within each type is comparable and sometimes exceeds the mean value of $\langle c_P \rangle$ for the given type of storm. One can say only that there is a tendency of D_{st} increase (weakening of the storm) with an increase in P_d for three types of storm (except MC).

The contribution of P_d to D_{st} (i.e., the value of $\langle c_P \rangle \cdot \langle P_d \rangle$ is maximum for the CIR- and Ejecta-induced storms (a strong weakening of the storm) and minimum for the Sheath-induced storms (weaker by a factor of ~2.5–3.5). An inverse effect (a very weak decrease in D_{st}, i.e., an intensification of the storm) is observed for the MC-induced storms. The large positive contribution of $\langle P_d \rangle$ to D_{st} for the CIR- and Ejecta-induced storms leads to a weakening (by 30–50%) of the contribution of the main parameter $\langle \text{sum}E_y \rangle$. Higher pressure $\langle P_d \rangle$ within these types of SW is a possible cause of this effect.

The $\langle c_B \rangle$ coefficient determines the efficiency of the contribution of the magnetic fluctuations sB in IMF into D_{st} at the main phase. On average, the value of $\langle c_B \rangle$ varies insignificantly for all types of SW, reducing slightly D_{st} and increasing the strength of a Sheath-induced storm and increasing slightly D_{st} and reducing the strength of a MC-induced storm.

The mean values of the fluctuations level $\langle sB \rangle$ correspond to physical conditions in SW types and vary from a minimum value for the MC-induced storms to a maximum value for the storms caused by the compression regions of the CIR- and Sheath-induced storms (that is, almost by a factor of 2 higher in the compression region, corresponding to the definition of the given type of streams).

The contribution of the fluctuation level $\langle sB \rangle$ into D_{st} is small (as compared to the contribution of $\langle \text{sum}E_y \rangle$ for all types of storms and depends on the type of SW. For the Sheath-induced storms, it reduces D_{st} intensifying the storm, whereas for the MC-induced storms, on the contrary, it increases D_{st} weakening the storm. The magnetic fluctuations intensify the storm slightly for the CIR- and Ejecta-induced storms.

Because of insufficiently high accuracy, the data shown in Table 1 by non-bold type could be interpreted in the following way: (1) for c_P the mean $\langle c_P \rangle \approx 0$ for MC and Sheath and (2) for c_B the mean $\langle c_B \rangle \approx 0$ for all types of SW. For these data the statistics should be increased and an additional analysis should be performed.

Thus the largest contributions to D_{st} of the main phase are provided by the $\langle c_0 \rangle$ parameters (by a factor of 2.4 higher for MC than for Ejecta) and the integral electric field sumE_y (by a factor of 1.4 higher for Sheath than for Ejecta), the value of which depends on the SW type. The contribution of the pressure P_d is the largest for CIR-induced and by a factor of 1.5 lower for the Ejecta-induced storms. For the Sheath-induced storms, the contribution of P_d is by a factor of 3.3 weaker than for the CIR-induced storms. For Ejecta the contribution of P_d weakens the storm (a positive c_P coefficient), whereas for MC the contribution of pressure intensifies the storm (a negative c_P coefficient). For all types of SW, the contribution of magnetic fluctuation level sB in IMF to D_{st} at the main phase is insignificant as compared to the main contribution from the sumE_y and its value presumably depends on the SW type. For the MC-induced storms, the fluctuations in IMF lead to a small increase in D_{st} of the phase (a weakening of the storm) which is almost compensated by a slight decrease in D_{st} (an intensification of the storm) due to the contribution of the pressure P_d. On the contrary, for the Sheath-induced storms, the fluctuations sB in IMF lead to a slight decrease in D_{st} (an intensification of the storm) which is almost compensated by a slight increase in D_{st} (a weakening of the storm) due to the contribution of the pressure P_d.

3.2. Comparison of Three Versions of Models of the Main Phase of Magnetic Storms Induced by Four Types of SW Streams

The dependence of the D_{st} index measured during the main phase on the model value $D_{st\,\text{mod}}$ calculated using individual approximation coefficients for each storm and four types of SW is shown in Fig. 1: (a) CIR, (b) Sheath, (c) MC, and (d) Ejecta. The correlation

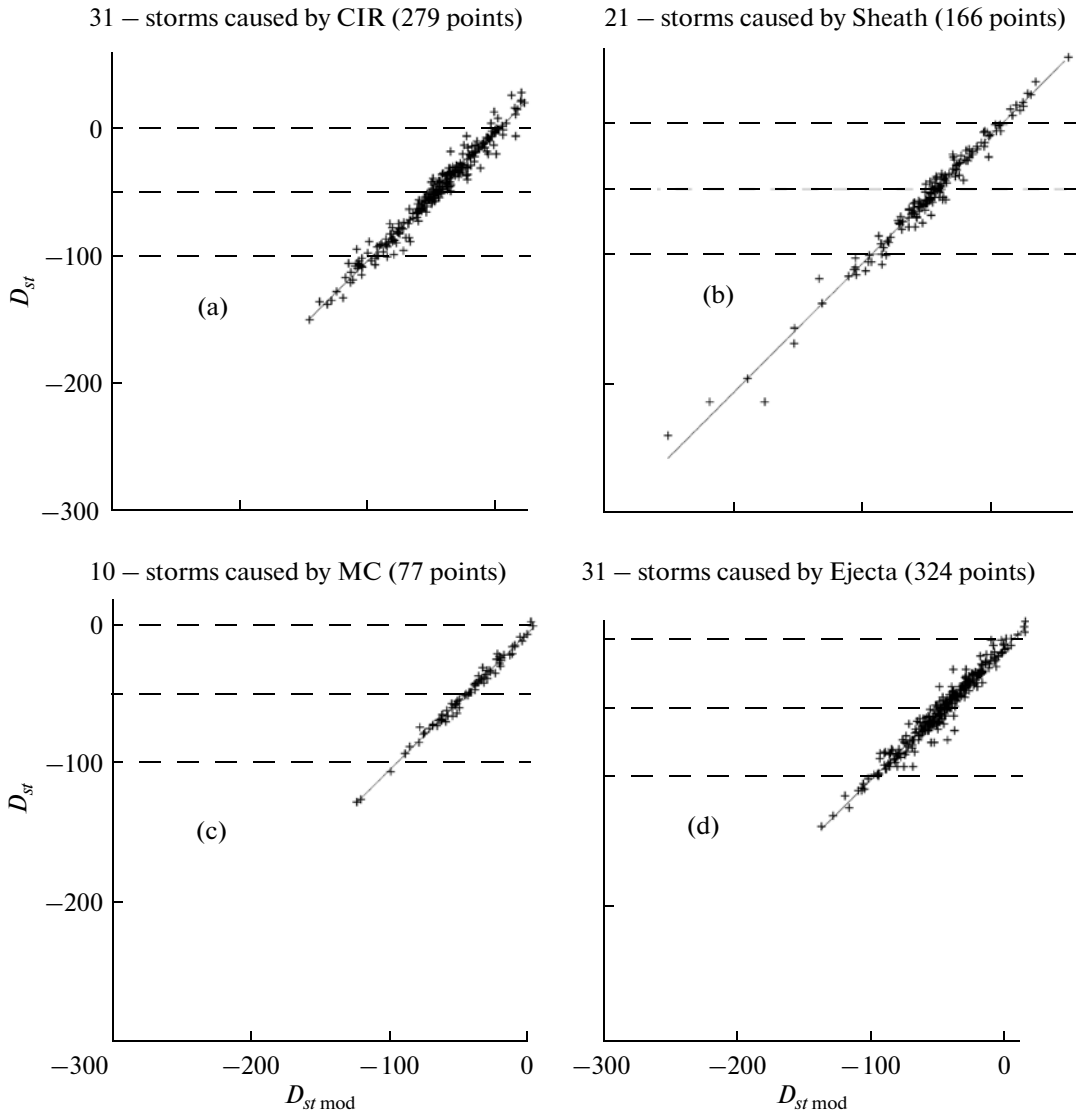

Fig. 1. The dependence of the D_{st} index measured during the main phase on the model value $D_{st\ \mathrm{mod}}$ calculated using individual approximation coefficients for each storm: (a) 31 CIR-induced storms; (b) 21 Sheath-induced storms; (c) 10 MC-induced storms; (d) 31 Ejecta-induced storms.

coefficients (r) and standard deviations (σ) as well as the lines of regression of D_{st} on $D_{st\,\mathrm{mod}}$ for three versions of models are shown in Table 2. Three bottom lines in the first column show the model versions: (1v) model with individual coefficients, (2v) model with averaged coefficients, and (3v) third model. For the model with individual approximation coefficients (1v) the correlation coefficient between D_{st} and $D_{st\,\mathrm{mod}}$ for all four types of SW is very high ($r = 0.98$ for the CIR- and Ejecta-induced storms and $r = 0.99$ for the MC- and Sheath-induced storms). The standard deviation is the lowest for the MC-induced storms, by a factor of two higher for the CIR- and Ejecta-induced storms, and is the highest for the Sheath-induced storms (the difference is a factor of 2.3). As expected, the individual coefficients obtained from an approximation for a particular storm provide the best result for modeling the main phase of a storm with any type of source in SW. Various storm types differ only by values of the correlation coefficients and σ. The current version of the model describes the main phase of the MC-induced storms [7] most accurately, but its accuracy is lower for the storms caused by Ejecta and Sheath by a factor of 2–2.3.

Figure 2 shows the same as in Fig. 1, but the model calculations of $D_{st\,\mathrm{mod}}$ are performed using the values of the approximation coefficients $\langle c_0\rangle$, $\langle c_E\rangle$, $\langle c_P\rangle$, $\langle c_B\rangle$, averaged over SW type (see Table 1). For this version of the model (2v), the correlation coefficient between the D_{st} values measured during the main phase and the modeled $D_{st\,\mathrm{mod}}$ and also the model accuracy decrease substantially for all types of SW. The highest correlation coefficient is for the storms caused by Sheath and

Table 2. The dependence of approximation coefficient c0 on (aveD_{st}) and measured D_{st} on $D_{st\ \mathrm{mod}}$ for 3 versions of models and for 4 types of SW streams

Type of SW / Values of parameters	MC 10 storms 77 points	Sheath 21 storms 116 points	CIR 31 storms 279 points	Ejecta 31 storms 324 points
c_0 on (aveD_{st})	$Y = 0.69 \cdot X - 6.51$	$Y = 0.26 \cdot X - 9.8$	$Y = 0.33 \cdot X - 26.15$	$Y = 0.4 \cdot X - 24.5$
r	0.730	0.239	0.233	0.292
(3v) D_{st} on (D_{st_mod})	$Y = 0.9 \cdot X + 0.84$	$Y = 0.8 \cdot X - 2.55$	$Y = 0.9 \cdot X - 6.5$	$Y = 0.7 \cdot X - 12.6$
σ	15.64	23.4	17.8	16.5
r	0.832	0.837	0.846	0.810
(2v) D_{st} on (D_{st_mod})	$Y = 0.68 \cdot X - 9.96$	$Y = 0.8 \cdot X - 3.5$	$Y = 0.9 \cdot X - 6.6$	$Y = 0.7 \cdot X - 12.6$
σ	21.74	26.2	20.1	18.4
r	0.648	0.804	0.803	0.758
(1v) D_{st} on (D_{st_mod})	$Y = 1.0 \cdot X + 2.445$	$Y = 1 \cdot X - 4 \times 10^{-8}$	$Y = 1.0 \cdot X - 5 \times 10^{-7}$	$Y = 1 \cdot X - 4.5 \times 10^{-6}$
σ	2.6	6.06	5.5	5.2
r	0.994	0.988	0.984	0.978

CIR, whereas the lower correlation coefficient is for the storms caused by MC (the difference is a factor of ~1.23). The Ejecta-induced storms have an intermediate value. The highest accuracy of the model (low σ) is for the Ejecta-induced storms. The lowest accuracy is for the storms caused by Sheath and MC (that is, a decrease in the accuracy by a factor of 1.4–1.2 as compared to Ejecta). In comparison to the previous version of the model (using individual coefficients), the reduction of the accuracy for the given types of SW is by a factor of ~4–8.

In order to increase the accuracy of the main phase modeling, we introduced corrections taking into account the prehistory of development of the beginning of the main phase of a magnetic storm [7]. Instead of a constant mean value of the $\langle c_0 \rangle$ coefficient, for each storm j (within the given type of SW) we took values of $c_0(j)$ calculated on the basis of the dependence of the $c_0(j)$ coefficient on the average value ave$D_{st}(j)$. This improved version of the model has the form:

$$D_{st\,mod}(i) = c_0(j) + \langle c_E \rangle \cdot \mathrm{sum}E_y(i)$$

$$+ \langle c_P \rangle \cdot P_d(i) + \langle c_B \rangle \cdot \mathrm{s}B(i), \text{ where } i \text{ is the point in the phase;}$$

$c_0(j) = a \cdot \mathrm{ave}D_{st}(j) + b$ (here ave$D_{st}(j)$ for the j storm of the given SW type is the average value over three points including two points prior to the storm commencement and the first point of the main phase of the storm, a and b are coefficients of approximation of the $c_0(j)$ dependence on ave$D_{st}(j)$, and the other coefficients $\langle c_E \rangle$, $\langle c_P \rangle$, $\langle c_B \rangle$ as earlier are taken from the averaging over all storms of the given SW type). Estimates of a possible relation of the $c_0(j)$ coefficients to the value of D_{st}, ave$D_{st}(j)$ averaged over three points (that is, the coefficients of correlation between them) and the approximation coefficients "a, b" are shown in the top line of Table 2. For 10 MC-induced storms, a linear dependence between these parameters $c_0 = 0.69 \cdot \mathrm{ave}D_{st} - 6.51$ is observed with a correlation coefficient of 0.73.

Figure 3 shows the D_{st} dependence on $D_{st\ \mathrm{mod}}$ for four types of storms for the third version of the $D_{st\ \mathrm{mod}}$ model when instead of a constant average value $\langle c_0 \rangle$ for each storm j values of $c_0(j)$ calculated using the above-mentioned linear dependence of the $c_0(j)$ coefficient on ave$D_{st}(j)$ are taken. One can see that this version of the model (3v) describes the experimental data better than the version with averaged coefficients (2v). The highest correlation coefficient is for the CIR-induced storms; it is slightly lower for the storms caused by Sheath and MC. The lowest correlation coefficient is for the storms caused by Ejecta (the difference in the r values is only ~1.05). The lowest value of the standard deviation is for the storms caused by MC and the highest standard deviation is for the storms caused by Sheath (they differ almost by a factor of 1.5). The storms caused by MC and Ejecta have similar values of σ.

4. DISCUSSION

Thus, we proposed and tested a model for description of the main phase of magnetic storms induced by four types of SW (10 MC-induced storms, 31 CIR-induced storms, 21 Sheath-induced storms, and 31 Ejecta-induced storms). The model is based on the assumption of linear dependence of D_{st} at the main phase on the integral electric field sumE_y, dynamic pressure P_d, and fluctuation level sB in IMF.

The analysis of results shows that the main contribution into the D_{st} index at the main phase is provided by the integral electric field sumE_y, which for all types of SW reduces the D_{st} value (intensifies the storm), the value of the reduction depending on the type of the storm source in SW. The strongest dependence of the D_{st} index on the integral electric field is observed for the Sheath-induced storms, this fact manifesting their

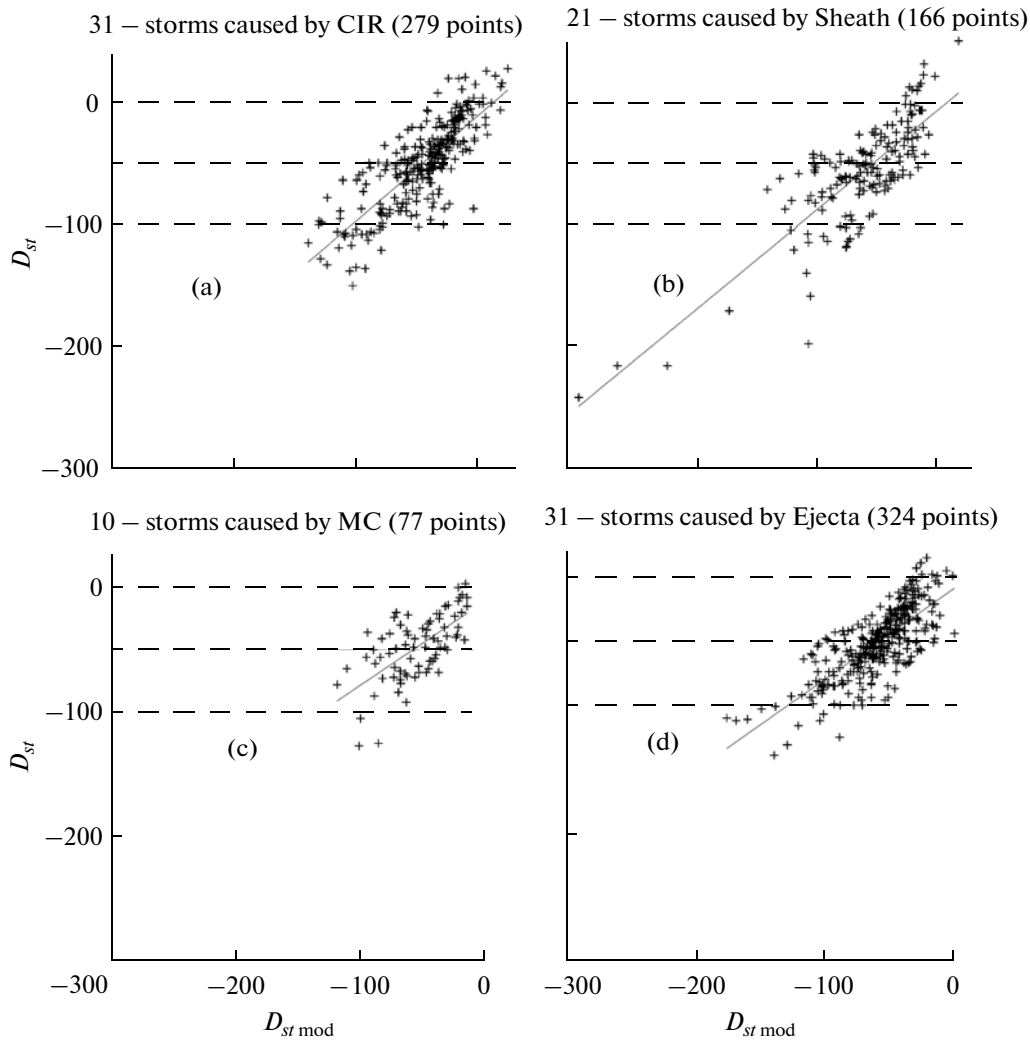

Fig. 2. The same as in Fig.1, but for model calculations of $D_{st\,\mathrm{mod}}$ the averaged by SW type values of the approximation coefficients were used.

higher efficiency (that is, ability to lead to stronger intensity of magnetic storms, $D_{st\,\mathrm{min}}$) as compared to other types of storms. This statement is confirmed by the sampling of storms caused by Sheath for which the intensity of a magnetic storm at its minimum reaches $D_{st\mathrm{min}} \sim -250$ nT (super-strong storms), whereas for other type of SW the value of $D_{st\,\mathrm{min}}$ during magnetic storms varies within more narrow range (from −50 to −150 nT). The higher intensity of the storms generated by Sheath was earlier noted qualitatively in [3, 35, 36, 39, 41, 47, 55–58]. However, in this paper, we, for the first time, present a numerical comparison of contributions (the $\langle c_E \rangle$ coefficients) for various interplanetary sources of storms.

The contribution of the dynamic pressure to D_{st} of the main phase also depends on the storm type. In particular, for two types of storms caused by MC and Sheath, the contribution of P_d is almost an order of magnitude less than the main contribution to D_{st} from sumE_y, and so it influences weakly D_{st} at the main phase (about 10%). At the same time, for two types of storms caused by CIR and Ejecta, the pressure P_d weakens the main phase of the storm by 30–50%.

The contribution of the fluctuation level sB in IMF to D_{st} at the main phase is small as compared to the contribution of sumE_y and also depends on the type of storm source. For example, for storms caused by CIR and Ejecta, it is a minimum and hardly influences D_{st} at the main phase (an intensification of the storm by 3%). For the storms caused by Sheath, it is a maximum (a factor of ~4 higher than for the CIR- and Ejecta-induced storms) and leads to (~10%) decrease in D_{st} at the phase (an intensification of the storm).

The third version of the model with the c_0 coefficient obtained from the c_0 dependence on D_{st} values in the preceding times prior to the storm beginning is characterized by higher values of the correlation coefficient between the measured D_{st} and $D_{st\,\mathrm{mod}}$ for Ejecta

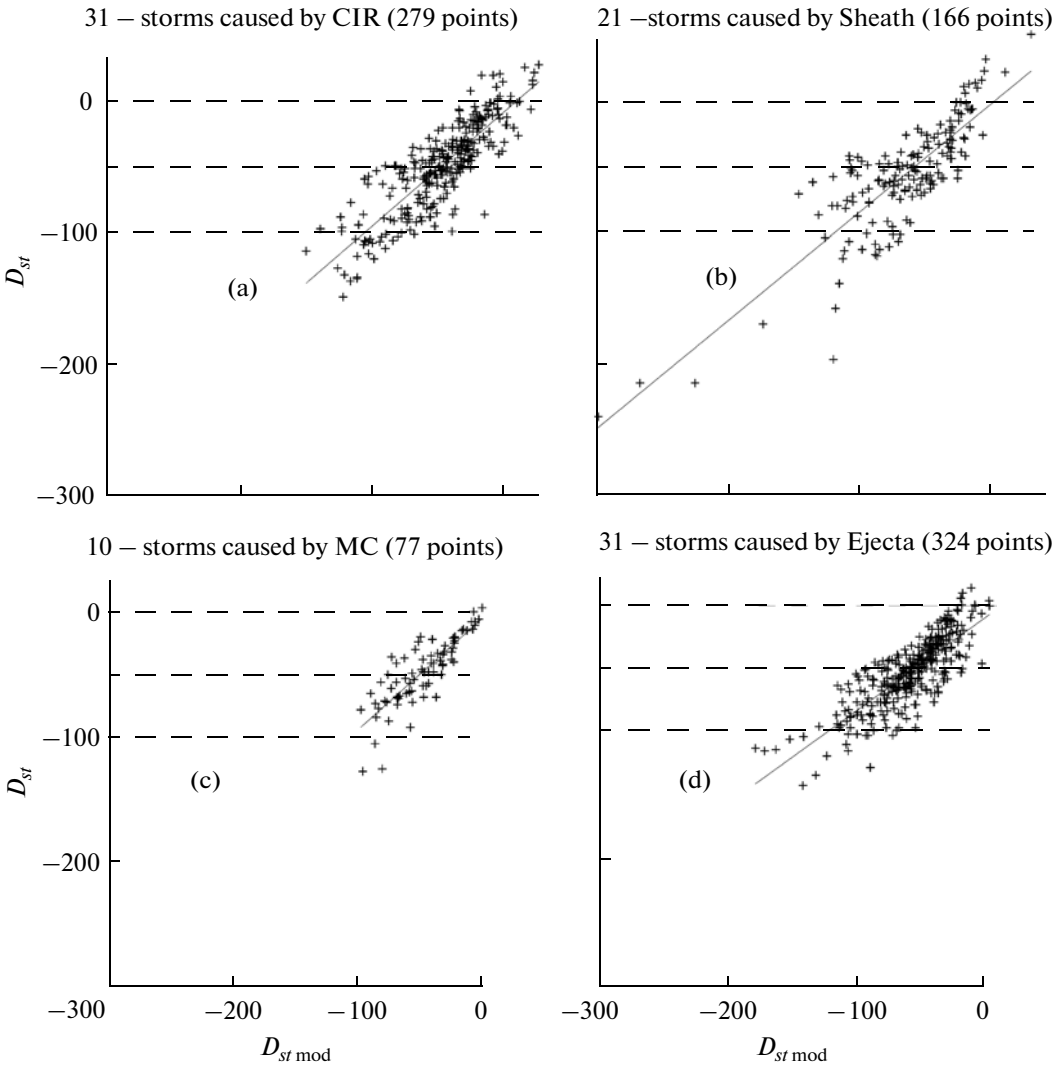

Fig. 3. The same as in Fig.1 and 2, but for model calculations of $D_{st\ \mathrm{mod}}$ the corrections taking into account the prehistory of development of the beginning of the main phase of a magnetic storm were used.

and CIR, and lower standard deviations for MC and Sheath, which is substantially better than for the model version with averaged approximation coefficients.

It is worth comparing our results obtained with the third model to the results of modeling the D_{st} index of magnetic storms separated by the SW type presented in other publications. Note that testing of various models should be performed using an independent set of data different from the data set used for the optimization of these models. Table 3 shows the correlation coefficients (r) and standard deviations for four types of SW and seven models including six models from [32] (which have been tested using a data set different from ours, see Introduction) and our third model (3v) taking into account the prehistory of D_{st} development prior to the beginning of the main phase.

Our third version of the model (3v) describes fairly well the main phase of storms for all types of SW. The value of the correlation coefficient (r) and the accuracy of the model (σ) depend on the SW type. For particular types of SW, our model could be better than many others, for some types it is, on the contrary, worse than other models. For example, the value of the correlation coefficient in our third model depends on the type of SW: (1) for the Sheath-induced storms it is better than all models except the TL model [27, 28], (2) for the MC and Ejecta models it coincides with the FL model [13] specially aimed at the MC-induced storms, but is worse than all other models including the B model [8]; (3) for the CIR-induced storms it is better than the B and FL models [8, 13] but worse than the other four models [14, 16, 31, 27, 28]. Similarly, concerning the accuracy (σ in nT) our third model: (1) for the MC-induced storms it is better than all models (including the TL model [27, 28]) and by a factor of three more accurate than the B and FL models [8, 13], (2) for the Sheath-induced storms it is better than

Table 3. The correlation coefficients and standard deviations for four types of SW streams and seven models

Models	MC		Sheath		CIR		Ejecta		References
	r	σ	r	σ	r	σ	r	σ	
3v	0.83	15.6	0.84	23.4	0.85	17.8	0.81	16.5	
B model	0.89	51.4	0.71	56.1	0.77	48.2	0.88	39.2	[8]
FL model	0.83	51.7	0.66	50.0	0.66	39.9	0.81	34.2	[13]
OM model	0.9	26.5	0.8	27.6	0.87	19.0	0.9	20.2	[14]
W model	0.91	22.4	0.81	25.4	0.87	16.2	0.92	15.3	[16]
TL model	0.94	18.5	0.92	12.5	0.95	11.8	0.94	11.8	[27, 28]
NM model	0.88	24.1	0.82	26.4	0.87	19.5	0.89	19.6	[31]

all models except the TL model (which is a factor of two more accurate than our model) [27, 28] and is by a factor of 2–2.5 more accurate than the B and FL models [8, 13], (3) for the CIR-induced storms it is better than all models except the TL model [27, 28] and by a factor of 2.2–2.7 more accurate than the B and FL models [8, 13], but a factor of 1.5 worse than the TL model [27, 28], (4) for the Ejecta-induced storms our model is better than four models but worse than the W and TL models [16, 27, 28] (which is a factor of 1.4 more accurate than our model) and by a factor of 2–2.4 more accurate than the B and FL models [8, 13].

Thus, the results of calculations using the third version of the model (with a correction for the storm beginning) agree with the experimental data and by their quality are no worse than the results of modeling by other authors.

5. CONCLUSIONS

The modeling of the main phase of 93 magnetic storms ($-250 < D_{st} < -50$ nT) for four types of SW, assuming a linear dependence of D_{st} on the parameters sumE_y, P_d, and sB in IMF, showed that the contribution of each parameter of the SW to D_{st}, as well as the correlation coefficient and accuracy of the model on average depend on the type of storm source in SW. However, the statistical significance of the coefficients for P_d and sB in IMF for some types of SW requires further investigations.

The modeling of the main phase is performed in three versions: (1) using individual approximation coefficients, (2) using the averaged approximation coefficients, and (3) using the averaged approximation coefficients as in case (2) but taking into account the prehistory of the development of the beginning of the main phase. The results of the analysis show that:

1) For all types of SW, the model version with individual approximation coefficients is the most accurate and describes in the best way the D_{st} variations during the main phase as compared to other models. Its accuracy depends on the SW type: the highest accuracy is for the storms caused by MC, the accuracy for the storms caused by Ejecta and CIR is lower by a factor of two, and the lowest accuracy (a factor of 2.3 lower) is for the storms caused by Sheath.

2) The largest contribution into D_{st} at the main phase of storms caused by various types of SW is provided by the integral electric field sumE_y. For the storms caused by Sheath, the contribution is higher (by a factor of 1.4), this fact being caused by higher efficiency of these interplanetary sources of storms relative to other types of SW.

3) The contribution of the dynamic pressure P_d to D_{st} at the main phase also depends on the SW type: the lowest contribution is for the MC- and Sheath-induced storms and it is higher for the CIR- and Ejecta-induced storms (it weakens D_{st} of storms by 30–50%).

4) The contribution of the fluctuations sB in IMF is small for all types of SW, but its value also depends on the SW type.

5) The third version of the model (with the correction for the storm beginning) is the best for a description of the development of the main phase of a storm for all types of SW, both for a description of variations in D_{st} and in accuracy. The correlation coefficient varies within the range from $r = 0.81$ for the storms caused by Ejecta to $r = 0.85$ for the storms caused by CIR. The highest and lowest accuracy is for the MC-induced storms (15.6 nT) and Sheath-induced storms (worse by a factor of 1.5), respectively.

6) The comparison to six models [8, 13, 14, 16, 27, 28, 31] from [32] shows that our third version of the model for the storms caused by MC and Ejecta is as good (by the correlation coefficient) as the FL model [13] (but worse than the other models [8, 14, 16, 27, 28, 31]). For the Sheath-induced storms it is better than almost all models except models [27, 28] and for the storms caused by CIR its efficiency is higher than that of the FL and B models [8, 13]. In accuracy our

third model is better for the MC-induced storms than almost all models including the TL model [27, 28], for the Sheath-induced storms is only worse than the TL model [27, 28], but is more accurate than five other models [8, 13, 14, 16, 31], and for the Ejecta- and CIR-induced storms is only worse than the TL and W models [16, 27, 28] but better than four other models [8, 13, 14, 31].

Thus it is shown that the contributions of the main parameters of SW into D_{st} at the main phase, the correlation coefficient between the measured D_{st} and modeled $D_{st\ \mathrm{mod}}$ values, and the accuracy of various versions of models depend on the SW type. The results agree with the earlier conclusions and confirm them quantitatively (for example, [3, 47]). We selected each of the SW types on the basis of certain physical criteria with various values of the SW parameters [51]. Moreover, in our sampling of storms with different type of SW, very strong storms ($-250 < D_{st\min} < -150$ nT) are present only in the sampling for the storms caused by Sheath. Nevertheless, the model (third version of the model) of the main phase for various types of SW rivals successfully other models both in the description of real variations in D_{st} and in accuracy (see [32] and references therein). Different coefficients of the model obtained for different interplanetary sources make it possible to forecast magnetic storms more accurately, analyzing in real time parameters of the interplanetary environment measured on board space vehicles of the type *Wind* or *ACE* [7].

ACKNOWLEDGMENTS

The authors are grateful for the use of the OMNI database. The OMNI data were taken from GSFC/SPDF OMNIWeb at the site http://omniweb.gsfc.nasa.gov. The work was supported by the Russian Foundation for Basic Research (projects Nos. 10-02-00277a and 13-02-00158a) and also by the Program No. P 22 of the Presidium of the Russian Academy of Sciences.

REFERENCES

1. Yermolaev, Yu.I., Lodkina, I.G., Nikolaeva, N.S., and Yermolaev, M.Yu., Statistical study of interplanetary condition effect on geomagnetic storms, *Kosm. Issled.*, 2010, vol. 48, no. 6, pp. 499–515. [*Cosmic Research*, pp. 485–500].
2. Yermolaev, Yu.I., Lodkina, I.G., Nikolaeva, N.S., and Yermolaev, M.Yu., Statistical study of interplanetary condition effect on geomagnetic storms: 2. Variations of parameters, *Kosm. Issled.*, 2011, vol. 49, no. 1, pp. 24–37. [*Cosmic Research*, pp. 21–34].
3. Yermolaev, Yu.I., Nikolaeva, N.S., Lodkina, I.G., and Yermolaev, M.Yu., Specific interplanetary conditions for CIR-, Sheath-, and ICME-induced geomagnetic storms obtained by double superposed epoch analysis, *Ann. Geophys.*, 2010, vol. 28, pp. 2177–2186.
4. Nikolaeva, N.S., Yermolaev, Yu.I., and Lodkina, I.G., Dependence of geomagnetic activity during magnetic storms on the solar wind parameters for different types of streams, *Geomagn. Aeron.*, 2011, vol. 51, no. 1, pp. 49–65.
5. Nikolaeva, N.S., Yermolaev, Yu.I., and Lodkina, I.G., Dependence of geomagnetic activity during magnetic storms on the solar wind parameters for different types of streams: 2. Main phase of storm, *Geomagn. Aeron.*, 2012, vol. 52, no. 1, pp. 28–36.
6. Nikolaeva, N.S., Yermolaev, Yu.I., and Lodkina, I.G., Geomagnetic activity during magnetic storms as a function of solar wind parameters for different types of flows: 3. Development of storm, *Geomagn. Aeron.*, 2012, vol. 52, no. 1, pp. 37–48.
7. Nikolaeva, N.S., Yermolaev, Yu.I., and Lodkina, I.G., Geomagnetic activity during magnetic storms as a function of solar wind parameters for different types of flows: 4. Modeling for magnetic clouds, *Geomagn. Aeron.*, 2013, no. 6. (in press).
8. Burton, R.K., McPherron, R.L., and Russell, C.T., An empirical relationship between interplanetary conditions and D_{st}, *J. Geophys. Res.*, 1975, vol. 80, pp. 4204–4214.
9. Kane, R.P., Severe geomagnetic storms and Forbush decreases: interplanetary relationships reexamined, *Ann. Geophys.*, 2010, vol. 28, pp. 479–489.
10. Ontiveros, V., Geomagnetic storms caused by shocks and ICMEs, *J. Geophys. Res.*, 2010, vol. 115, A10244. doi: 10.1029/2010JA015471.
11. Weigel, R.S., Solar wind density influence on geomagnetic storm intensity, *J. Geophys. Res.,* 2010, vol. 115, A09201. doi: 10.1029/2009JA015062.
12. Feldstein, Y.I., Modelling of the magnetic field of magnetospheric ring current as a function of interplanetary parameters, *Space Sci. Rev.*, 1992, vol. 59, pp. 83–165.
13. Fenrich, F.R. and Luhmann, J.G., Geomagnetic response to magnetic clouds of different polarity, *Geophys. Res. Lett.*, 1998, vol. 25, pp. 2999–3002.
14. O'Brien, T.P. and McPherron, R.L., An empirical phase space analysis of ring current dynamics: Solar wind control of injection and decay, *J. Geophys. Res.*, 2000, vol. 105, pp. 7707–7720.
15. O'Brien, T.P. and McPherron, R.L., Forecasting the ring current index D_{st} in real time, *J. of Atmosph. and Sol.-Terrestr. Phys.*, 2000, vol. 62, pp. 1295–1299.
16. Wang, C.B., Chao, J.K., and Lin, C.-H., Influence of the solar wind dynamic pressure on the decay and injection of the ring current, *J. Geophys. Res.*, 2003, vol. 108, no. A9, p. 1341. doi: 10.1029/2003JA009851.
17. Maltsev, Y.P., Points of controversy in the study of magnetic storms, *Space Sci. Rev.*, 2004, vol. 110, pp. 227–267.
18. Siscoe, G., McPherron, R.L., Liemohn, M.W., Ridley, A.J., and Lu, G., Reconciling prediction algorithms for D_{st}, *J. Geophys. Res.*, 2005, vol. 110, A02215. doi: 10.1029/2004JA010465.
19. Podladchikova, T.V. and Petrukovich, A.A., Extended geomagnetic storm forecast ahead of available solar wind measurements, *Space Weather*, 2012, vol. 10, S07001. doi: 10.1029/2012SW000786.
20. Vassiliadis, D., Klimas, A.J., Baker, D.N., and Roberts, D.A., A description of solar wind–magneto-

sphere coupling based on nonlinear filters, *J. Geophys. Res.*, 1995, vol. 100, no. A3, pp. 3495–3512.

21. Vassiliadis, D., Klimas, A.J., and Baker, D.N., Models of D_{st} geomagnetic activity and of its coupling to solar wind parameters, *Phys. Chem. Earth (C)*, 1999, vol. 24, nos. 1-3, pp. 107–112.
22. Vassiliadis, D., Klimas, A.J., Valdivia, J.A., and Baker, D.N., The D_{st} geomagnetic response as a function of storm phase and amplitude and the solar wind electric field, *J. Geophys. Res.*, 1999, vol. 104, no. A11, pp. 24957–24976.
23. Klimas, A.J., Vassiliadis, D., Baker, D.N., and Roberts, D.A., The organized nonlinear dynamics of the magnetosphere, *J. Geophys. Res.*, 1996, vol. 101, pp. 13089–13113.
24. Klimas, A.J., Vassiliadis, D., and Baker, D.N., D_{st} index prediction using data-derived analogues of the magnetospheric dynamics, *J. Geophys. Res.*, 1998, vol. 103, pp. 20435–20447.
25. Wu, J.-G. and Lundstedt, H., Neural network modeling of solar wind-magnetosphere interaction, *J. Geophys. Res.*, 1997, vol. 102, no. A7, pp. 14457–14466.
26. McPherron, R.L. and O'Brien, T.P., Predicting geomagnetic activity: the D_{st} index, in *Space Weather*, vol. 125 of Geophys. Monogr. ser., Song, P., Singer, H.J., and Siscoe G.L., Eds., Washington, DC: AGU, 2001.
27. Temerin, M. and Li, X., A new model for the prediction of dst on the basis of the solar wind, *J. Geophys. Res.,* 2002, vol. 107, no. A12, p. 1472.
28. Temerin, M. and Li, X., D_{st} model for 1995–2002, *J. Geophys. Res.*, 2006, vol. 111, A04221. doi: 10.1029/2005JA011257.
29. Sharifi, J., Araabi, B.N., and Lucas, C., Multi-step prediction of D_{st} index using singular spectrum analysis and locally linear neurofuzzy modeling, *Earth Planets Space*, 2006, vol. 58, pp. 331–341.
30. Amata, E., Pallocchia, G., Consolini, G., Marcucci, M.F., and Bertello, I., Comparison between three algorithms for D_{st} predictions over the 2003–2005 period, *J. of Atmosph. and Sol.-Terrest. Phys.*, 2008, vol. 70, pp. 496–502.
31. Boynton, R.J., Balikhin, M.A., Billings, S.A., Sharma, A.S., and Amariutei, O.A., Data derived NARMAX D_{st} model, *Ann. Geophys.*, 2011, vol. 29, pp. 965–971.
32. Ji, E.-Y., Moon, Y.-J., Gopalswamy, N., and Lee, D.-H., Comparison of D_{st} forecast models for intense geomagnetic storms, *J. Geophys. Res.*, 2012, vol. 117, A03209. doi: 10.1029/2011JA016872.
33. Borovsky, J.E. and Denton, M.H., Differences between CME-driven storms and CIR-driven storms, *J. Geophys. Res.*, 2006, vol. 111, A07808. doi: 10.1029/2005JA011447.
34. Denton, M.H., Borovsky, J.E., Skoug, et al., Geomagnetic storms driven by ICME and CIR-dominated solar wind, *J. Geophys. Res.,* 2006, vol. 111, A07S07. doi: 10.1029/2005JA011436.
35. Huttunen, K.E.J., Koskinen, H.E.J., Karinen, A., and Mursula, K., Asymmetric development of magnetospheric storms during magnetic clouds and sheath regions, *Geophys. Res. Lett.,* 2006, vol. 33, p. L06107. doi: 10.1029/2005GL027775.
36. Pulkkinen, T.I., Partamies, N., Huttunen, K.E.J., Reeves, G.D., and Koskinen, H.E.J., Differences in geomagnetic storms driven by magnetic clouds and ICME sheath regions, *Geophys. Res. Lett.*, 2007, vol. 34, L02105. doi: 10.1029/2006GL027775.
37. Plotnikov, I.Ya. and Barkova, E.S., Nonlinear dependence of D_{st} and A_e indices on the electric field of magnetic clouds, *Adv. Space Res.*, 2007, vol. 40, pp. 1858–1862.
38. Longden, N., Denton, M.H., and Honary, F., Particle precipitation during ICME-driven and CIR-driven geomagnetic storms, *J. Geophys. Res.,* 2008, vol. 113, p. A06205. doi: 10.1029/2007JA012752.
39. Turner, N.E., Cramer, W.D., Earles, S.K., and Emery, B.A., Geoefficiency and energy partitioning in CIR-driven and CME-driven storms, *J. of Atmosph. and Sol.-Terrest. Phys.*, 2009, vol. 71, pp. 1023–1031.
40. Despirak, I.V., Lubchich, A.A., and Guineva, V., Development of substorm bulges during storms of different interplanetary origins, *J. of Atmosph. and Sol.-Terrest. Phys.*, 2011, vol. 73, pp. 1460–1464.
41. Guo, J., Feng, X., Emery, B.A., et al., Energy transfer during intense geomagnetic storms driven by interplanetary coronal mass ejections and their sheath regions, *J. Geophys. Res.*, 2011, vol. 116, A05106. doi: 10.1029/2011JA016490.
42. Tsurutani, B.T., Lakhina, G.S., Pickett, J.S., Guarnieri, F.L., Lin, N., and Goldstein, B.E., Nonlinear Alfven's waves, discontinuities, proton perpendicular acceleration, and magnetic holes/decreases in interplanetary space and the magnetosphere: Intermediate shocks?, *Nonlinear Proc. Geophys.,* 2005, vol. 12, p. 321.
43. Jordanova, V.K., Modeling the behavior of corotating interaction region driven storms in comparison with coronal mass ejection driven storms, in *Recurrent Magnetic Storms: Corotating Solar Wind Streams*, Tsurutani, B.T., McPherron, R.L., Gonzalez, W.D., Lu, G., Sobral, J.H.A., and Gopalswamy, N., Eds., vol. 167 of Geophysical Monograph Series, Washington, DC: AGU, 2006.
44. Liemohn, M.W. and Jazowski, M., Ring current simulations of the 90 intense storms during solar cycle 23, *J. Geophys. Res.*, 2008, vol. 113, p. A00A17. doi: 10.1029/2008JA013466.
45. Liemohn, M.W., Jazowski, M., Kozyra, J.U., Ganushkina, N., Thomsen, M.F., and Borovsky, J.E., CIR versus CME drivers of the ring current during intense magnetic storms, *Proc. R. Soc. A,* 2010, vol. 466, pp. 3305–3328. doi: 10.1098/rspa.2010.0075.
46. Cerrato, Y., Saiz, E., Cid, C., Gonzalez, W.D., and Palacios, J., Solar and interplanetary triggers of the largest D_{st} variations of the solar cycle 23, *J. of Atmosph. and Sol.-Terrest. Phys.,* 2012, vol. 80, pp. 111–123.
47. Yermolaev, Yu.I., Nikolaeva, N.S., Lodkina, I.G., and Yermolaev, M.I., Geoeffectiveness and efficiency of CIR, Sheath, and ICME in generation of magnetic storms, *J. Geophys. Res.*, 2012, vol. 117, p. A00L07. doi: 10.1029/2011JA017139.
48. Tsyganenko, N.A. and Sitnov, M.I., Modeling the dynamics of the inner magnetosphere during strong

geomagnetic storms, *J. Geophys. Res.*, 2005, vol. 110, p. A03208. doi: 10.1029/2004JA010798.

49. Levitin, A.E., Dremukhina, L.A., Gromova, L.I., and Ptitsyna, N.G., Modeling giant disturbances in geomagnetic field, *Physics of Auroral Phenomena, Proc. XXXIV Annual Seminar, Apatity, 2011*, pp. 29–32.

50. King, J.H. and Papitashvili, N.E., Solar wind spatial scales in and comparisons of hourly wind and ace plasma and magnetic field data, *J. Geophys. Res.,* 2004, vol. 110, no. A2, p. A02209. doi: 10.1029/2004JA010804.

51. Yermolaev, Yu.I., Nikolaeva, N.S., Lodkina, I.G., and Yermolaev, M.Yu., Catalog of Large-Scale Solar Wind Phenomena during 1976-2000, *Kosm. Issled.,* 2009, vol. 47, no. 2, pp. 99–113. [*Cosmic Research*, pp. 81–94].

52. Garcia, H.A. and Dryer, M., The solar flares on February 1986 and the ensuing intense geomagnetic storm, *Solar Phys.*, 1987, vol. 109, pp. 119–137.

53. Tsurutani, B.T., Gonzalez, W.D., Tang, F., and Lee, E.T., Great magnetic storms, *Geophys. Res. Lett.*, 1992, vol. 19, no. 1, pp. 73–76.

54. Eselevich, V.G. and Fainshtein, V.G., An investigation of the relationship between the magnetic storm D_{st}-index and different types of solar wind streams, *Ann. Geophys.*, 1993, vol. 11, no. 8, pp. 678–684.

55. Huttunen, K.E.J. and Koskinen, H.E.J., Importance of post-shock streams and sheath region as drivers of intense magnetospheric storms and high-latitude activity, *Ann. Geophys.*, 2004, vol. 22, pp. 1729–1738.

56. Yermolaev, Y.I., Yermolaev, M.Y., Lodkina, I.G., and Nikolaeva, N.S., Statistic investigation of heliospheric conditions resulting in magnetic storms, *Kosm. Issled.*, 2007, vol. 45, no. 1, pp. 3–11. [*Cosmic Research*, pp. 1–8].

57. Yermolaev, Y.I., Yermolaev, M.Y., Lodkina, I.G., and Nikolaeva, N.S., Statistic investigation of heliospheric conditions resulting in magnetic storms: 2, *Kosm. Issled.*, 2007, vol. 45, no. 6, pp. 489–498. [*Cosmic Research*, pp. 461–470].

58. Yermolaev, Y.I., Yermolaev, M.Y., Nikolaeva, N.S., and Lodkina, L.G., Interplanetary conditions for CIR-induced and MC-induced geomagnetic storms, *Bulg. J. Phys.*, 2007, vol. 34, pp. 128–135.

Translated by A. Danilov